Received: 13 October 2022 | Revised: 9 December 2022 | Accepted: 27 December 2022

DOI: 10.1002/psc.3477

RESEARCH ARTICLE

Journal of PeptideScience WILEY

Towards a templated reaction that translates RNA in cells into a proaptotic peptide-PNA conjugate

Yannic Altrichter | Peter Bou-Dib | Christina Kuznia | Oliver Seitz

Department of Chemistry, Humboldt University Berlin, Berlin, Germany

Correspondence
Oliver Seitz, Department of Chemistry, Humboldt University Berlin, Brook-Taylor-Str. 2, Berlin 12489, Germany.
Email: oliver.seitz@chemie.hu-berlin.de

Funding information
European Research Council's Horizon 2020, Grant/Award Number: ERC AdG TRIGGDRUG / 669628

Nucleic acid-templated chemistry opens the intriguing prospect of triggering the synthesis of drugs only in diseased cells. Herein, we explore the feasibility of using RNA-templated chemical reactions for the activation of a known Smac peptidomimetic compound (SMC), which has proapoptotic activity. Two peptide nucleic acid (PNA) conjugates were used to enable conditional activation of a masked SMC by reduction of an azide either by Staudinger reduction or catalytic photoreduction using a ruthenium complex. The latter provided ~135 nM SMC-PNA on as little as 10 nM (0.01 eq.) template. For the evaluation of the templated azido-SMC reduction system *in cellulo*, a stable HEK 293 cell line was generated, which overexpressed a truncated, non-functional form of the XIAP mRNA target. We furthermore describe the development of electroporation protocols that enable a robust delivery of PNA conjugates into HEK 293 cells. The action of the reactive PNA conjugates was evaluated by viability and flow cytometric apoptosis assays. In addition, electroporated probes were re-isolated and analyzed by ultra-high performance liquid chromatography (UPLC). Unfortunately, the ruthenium-PNA conjugate proved phototoxic, and treatment of cells with PNA-linked reducing agent and the azido-masked SMC conjugate did not result in a greater viability loss than treatment with scrambled sequence controls. Intracellular product formation was not detectable. A control experiment in total cellular RNA isolate indicated that the templated reaction can in principle proceed in a complex system. The results of this first-of-its-kind study reveal the numerous hurdles that must be overcome if RNA molecules are to trigger the synthesis of pro-apoptotic drugs inside cells.

KEYWORDS
apoptosis, cellular delivery, DNA-templated synthesis, peptide nucleic acid, photocatalysis, RNA, synthesis, templated chemistry

Abbreviations: Ahx, 6-aminohexanoic acid; asc, ascorbic acid; BIR, baculovirus IAP repeat; bpy, 2,2′-bipyridine; CHAPS, 3-[(3-cholamidopropyl)dimethyl-ammonio]-1-propanesulfonate; Chg, L-2-cyclohexylglycine; Dap, 2,3-diaminopropanoic Acid; Dip, L-diphenylalanine; DMEM, Dulbecco's modified Eagle's medium; dmTCEP, 3-bis(3-methoxy-3-oxopropyl)phosphanylpropanoic acid; EDTA, 2,2′,2″,2‴-(ethane-1,2-diyldinitrilo)tetraacetic acid; FAM, 6-carboxyfluorescein; IAP, inhibitor of apoptosis protein; mcbpy, 4′-methyl-4-carboxy-2,2′-bipyridine; MOPS, 3-morpholinopropane-1-sulfonic acid; NCL, native chemical ligation; NLS, nuclear localization signal; PBS, phosphate-buffered saline; PNA, peptide nucleic acid; SDS, sodium dodecylsulfate; Smac, second mitochondria-derived activator of caspases; SMC, Smac peptidomimetic compound; UPLC, ultra-high performance liquid chromatography; WT, wild-type; XIAP, X-linked inhibitor of apoptosis protein.

In Memory of Ulf Diederichsen (1963–2021).

Parts of this article are extracted from the dissertation of Yannic Altrichter: Y. Altrichter, *Degree Thesis*, Humboldt-Universität zu Berlin, **2022**.

1 | INTRODUCTION

Targeted tumor therapy seeks to exploit molecular differences between healthy and malignant cells to increase drug specificity and limit undesired perturbations of healthy cells. A hallmark of cancer is the accumulation of DNA sequence alterations and changed expression patterns, for example, of molecules involved in signal transduction and/or regulation of apoptosis. Thus, the genetic information of a cell represents a fundamental marker for the presence of disease. However, most available drugs act on proteins rather than nucleic acids.[1] Nucleic acid-templated reactions offer a way to translate the recognition of genetic information into a therapeutic principle acting on proteins (Figure 1A).[2,3] Such a templated reaction would only proceed in diseased cells expressing disease-specific RNA molecules and instruct the formation or activation of a peptide that antagonizes a protein critically involved in cancer.

The idea to use cellular RNA molecules as triggers for drug synthesis[4] requires methods that couple RNA recognition with a change of chemical reactivity. Reactive molecules must be able to "read" and "translate" the sequence of an RNA molecule into a drug-like output. A diverse set of nucleic acid programmed chemical reactions is available for applications in diverse areas such as nucleic acid detection/imaging,[5,6] DNA nanotechnology,[7] and DNA-encoded libraries.[8,9] Commonly, oligonucleotides are used for recognition of DNA and RNA templates. For reactions involving peptides, the use of peptide nucleic acid (PNA) is attractive (Figure 1B). PNA is an oligomer of aminoethylglycine that has carboxymethylated nucleobases scaffolded to the glycine amino group via amide bonds.[10–12] Its peptidic nature facilitates combination of nucleic acid recognition motifs and peptides in one molecule.[13–15] First examples demonstrating the use of PNA in templated chemistry have been contributed by the groups of Orgel,[16] Taylor,[17] and our group.[18,19] Cai et al. had proposed to use nucleic acid templated reactions for the release of drugs and used phosphine-induced Staudinger reduction of azido-dyes as a model (Figure 2A).[20] Our work focused on templated peptide coupling reactions such as the native chemical ligation[21] (NCL, Figure 2B).[22–33] Very recently, we extended the scope of NCL chemistry to the DNA/RNA-encoded synthesis of receptor tyrosine kinase inhibitors.[34] We, and others, sought reactions that proceed with turnover in template.[30,35,36] This is a desired feature as the catalytic efficiency provides a means of amplification, which increases the sensitivity for nucleic acid detection. Turnover is also important for the envisaged templated synthesis/activation of drug molecules in diseased cells because the proteins targeted by drugs are usually expressed in higher copy numbers than the targeted mRNA. To improve upon turnover, we introduced templated acyl transfer reactions[26] (Figure 2C) and applied them to DNA- and RNA-templated peptide synthesis.[29,37–39] In a notable example, we demonstrated alanine transfer reactions forming a tetrapeptide motif known to antagonize the X-linked inhibitor of apoptosis protein (XIAP).[29] Using exogenously added DNA template, the reaction proceeded in cell lysate and the formed product proved able to restore the activity of caspases. In another example, the synthesis of a cytotoxic peptide was put under the control of an RNA template.[37] The reaction outside cells established a cell-penetrating peptide, which enabled delivery of the cytotoxic peptides into cells. The Winssinger group focused on the development of templated reactions proceeding with high speed. After initial work involving phosphine-induced reduction of azido dyes,[40] Gorska et al. published a method that allows the release of estradiol (Figure 2D).[41] They also developed the [Ru^{2+}]-catalyzed photoreductive cleavage of azido-dyes (Figure 2E)[42] and *N*-picolinium-quenched dyes (Figure 2F).[43] We took advantage of this chemistry in new reaction formats inducing cleavage of nucleic acid probes.[44,45] The [Ru]-photocatalyzed reduction of *N*-picolinium groups as well as the recently reported templated PNA ligation via selenoester methodology[46] proceeds at remarkably high speed (Figure 2H). Diederichsen used PNA-PNA recognition to direct the NCL of two peptides (Figure 2G) and photocleavable linkers to enable the removal of the PNA units after ligation.[47]

In spite of the variety of template-controlled reactions of PNA-peptide hybrids that have been reported, the formation of a bioactive peptide in living cells instructed by endogenous RNA molecules remained an elusive goal. In this report, we describe our efforts to

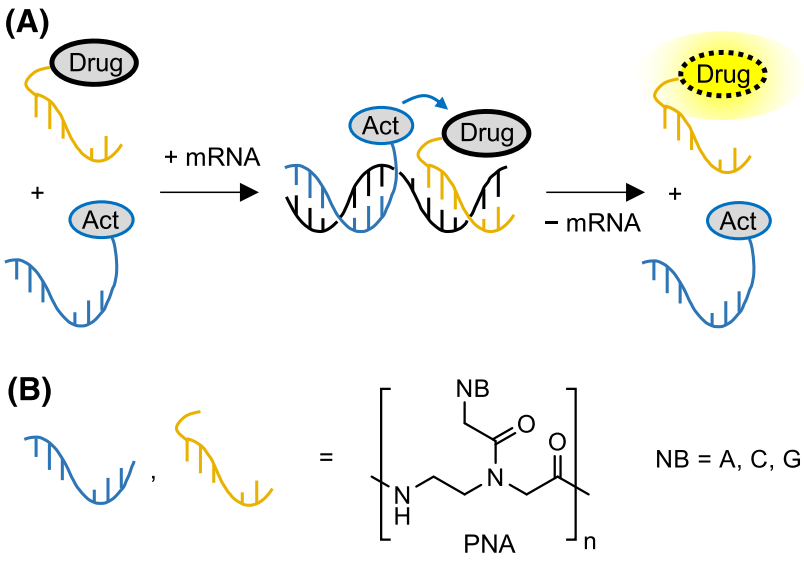

FIGURE 1 Principle of a mRNA-triggered activation of drug-nucleic acid conjugates. Act = generic reagent inducing drug activation; NB = nucleobase

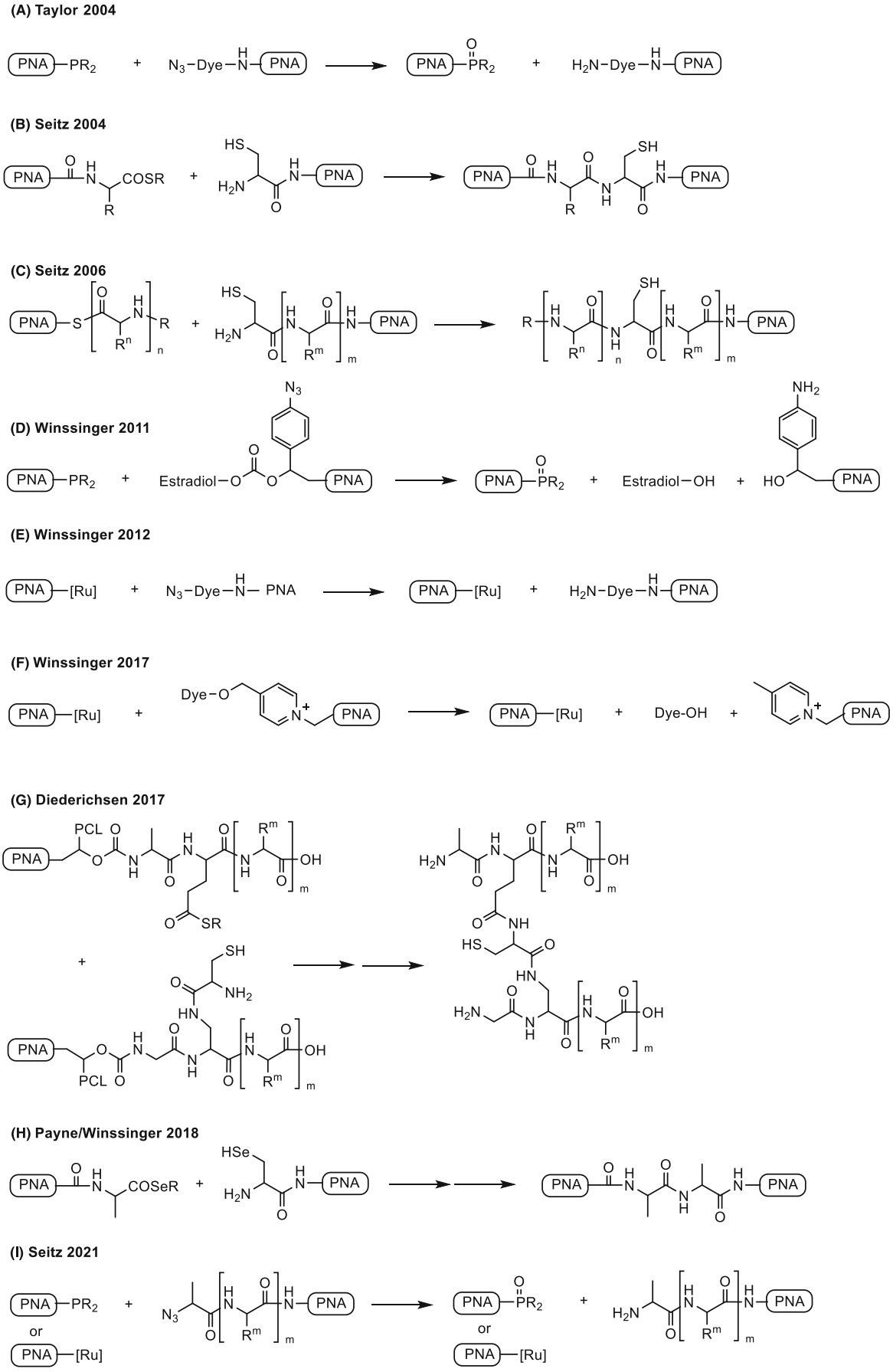

FIGURE 2 Overview of templated reactions with PNA applicable for drug activation

achieve this aim. For this purpose, we took recourse to a recently described reaction (Figure 2I), which restores the *N*-terminal amino group of an azide-modified Smac peptidomimetic compound (SMC).[48] SMCs are based on the AVPI tetrapeptide found at the N-terminus of the second mitochondria-derived activator of caspases (Smac).[49–51] These compounds have pro-apoptotic activity because they bind the IAP baculoviral repeat (BIR) domains of IAPs and thereby prevent action of IAP on caspases. Their *N*-terminal amino group is a requirement for high affinity interactions with the BIR domains,[52,53] and consequently, azido-SMCs have negligible binding affinity.[48] In addition to having introduced a templated reaction inducing the reduction of a PNA-linked azido-SMC, we have demonstrated the pro-apoptotic activity of nucleic acid-SMC conjugates.[54] Herein, we describe an exploration of the templated azido-SMC reduction in live cells. We assessed reductions induced by a PNA-linked phosphine and reactions photocatalyzed by a PNA-linked ruthenium complex. Furthermore, the study included the construction of cell lines expressing mRNA targets at defined levels, optimization of cellular delivery, establishment of viability/apoptosis assays, and methods for re-extraction of cell-delivered compounds for detection of reaction products by high-performance liquid chromatography (HPLC) analysis. The results point to the potential pitfalls that can be encountered when RNA molecules are supposed to trigger the synthesis of pro-apoptotic drugs inside cells.

2 | MATERIALS AND METHODS

2.1 | Materials

Unless specified, all reagents and solvents were of analytical grade or the highest available purity. A detailed list of chemicals is available in the Supporting Information. Chemicals not listed were ordered from Sigma-Aldrich (Ward Hill, MA, USA) or TCI Deutschland (Eschborn, Germany). Micro reaction vessels and centrifuge tubes were ordered from Sarstedt (Nümbrecht, Germany). Ultrapure water for HPLC, preparation of buffers, and dissolution of conjugates was prepared with an Astacus system (membraPure, Henningsdorf, Germany). Primers, XIAP amplicon, and RNA templates were obtained from Biomers.net GmbH (Ulm, Germany). A detailed list of kits, cell culture supplies, and molecular biology materials is available in the Supporting Information. The synthesis of the PNA conjugates dmTCEP, Ru, and N3 was described previously.[48] The synthesis of scrambled sequence control PNA conjugate scr and labeled PNA conjugates N3_biot, scr_biot, and H2N_biot is described in the Supporting Information.

2.2 | Templated reactions in buffer

Templated reactions were performed in degassed 3-morpholinopropane-1-sulfonic acid (MOPS) buffer (10 mM MOPS, 200 mM NaCl, 0.1% [w/v] CHAPS, pH 7.0) and analyzed by reversed-phase ultra-high performance liquid chromatography (RP-UPLC) (System A, Column 3; see Table S4 for details). Reactions were performed in poplypropylene microvolume inserts (dmTCEP probes) or black, non-binding 96-well F-bottom plates (Ru(II)-probes) at 25°C or 37°C using a thermoshaker or a custom-built multiwell plate heating element connected to a thermostat. For reactions with the dmTCEP-PNA conjugate, a stock solution of N_3-SMC-PNA (2 μM) and stoichiometric/substoichiometric amounts of RNA or 2′OMe RNA template (1, 0.3, 0.1, 0.03, 0.01, or 0 eq.) in (preheated) buffer was prepared. One volume of dmTCEP probe (4 or 6 μM) in tempered buffer was added (final concentration N_3-SMC-PNA probe: 1 μM, dmTCEP probe: 2 μM), and the mixture allowed to react for up to 6 h. For reactions with the Ru(II)-PNA, 5 mM ascorbic acid was added to the buffer. The stock solution of N_3-SMC-PNA (2 μM) and RNA template (1, 0.3, 0.1, 0.03, 0.01, or 0 eq.) in buffer was prepared and added to the wells of a non-binding 96-well plate. An equal volume of Ru(II)-PNA (4 or 6 μM) in buffer was added, the plate sealed with EASYseal™ adhesive sealer (Greiner Bio-One, Kremsmünster, Austria) and incubated for 10 min in the dark. The wells were then irradiated ($\lambda = 455$ nm, 1 W) using a M455L3-C1 collimated LED lamp mounted 15 cm above the plate and controlled by a DC2200 LED driver (Thorlabs, Newton, NJ, USA). At different time points (0, 1, 2, 3.5, 5, 7.5, 10, 15, 20, 40, 60, and 90 min), the irradiation was paused, 25 μl aliquots were taken, placed in poplypropylene microvolume inserts, and analyzed by RP-UPLC. The plate was resealed and the irradiation continued. Conversion was calculated from the area under the curve obtained by measuring absorption at $\lambda = 260$ nm.

2.3 | Cell culture

HEK 293 and Jurkat cell lines were maintained at 37°C in a humidified 5% CO_2 atmosphere and sub-cultivated in T-75 flasks twice a week. Cells were cultured in DMEM, supplemented with 10% (v/v) heat-inactivated fetal calf serum (FCS), 1% (v/v) Penicillin/Streptomycin mixture (100 U/ml) and 0.5 mM L-glutamine. Stable, XIAP-overexpressing cell lines HEK 293-XIAP and Jurkat-XIAP were cultured in the presence of 3 μg/ml puromycin selection antibiotic. For passaging and plating, cells in the exponential growth phase were washed with phosphate-buffered saline (PBS) buffer (137 mM NaCl, 2.7 mM KCl, 10 mM Na_2HPO_4, 1.8 mM KH_2PO_4, pH 7.4) and detached with Trypsin–EDTA solution (0.25%) for 3–5 min at 37°C (only HEK 293 cells). Cells were taken up in DMEM, centrifuged (5 min, 200 × g) and suspended in fresh medium before being plated or passaged to new cultivation flasks. Cell density was determined using a Countess™ II automated cell counter (Thermo Fisher Scientific, Waltham, MA, USA).

2.4 | Generation of stable cell lines

Stable cell lines were created by using the CRISPR/Cas9 Genome Knockout Kit (OriGene Technologies, Rockville, MD, USA) and donor vector pAAVS1-mCherry(NLS)-P2A-XIAP (see Supporting Information

for plasmid map) generated through Gibson assembly with the manufacturer's commercially available pAAVS1-Puro-DNR vector (see Table S1 for sequence). The target sequence-containing P2A-XIAP (43–109) fragment was amplified by polymerase chain reaction (PCR) from a pcDNA3.1-XIAP ORF clone vector (accession number NM_001167.3; Biozol, Eching, Germany), the mCherry(NLS) fragment from a plasmid (mCherry-Ftag)[55] constructed by Dr. Dhana Friedrich (Alexander Löwer Group, Technical University Darmstadt, Germany). The sequence overlaps for Gibson assembly were introduced with primer overhangs. For each fragment, 10 ng template was mixed with 25 µl 2× Q5® High-Fidelity 2X Master Mix (new England Biolabs, Ipswich, MA, USA) and 500 nM (final concentration) P2A-XIAP(43–109) or mCherry(NLS) forward and reverse primer, respectively (for sequences see Table S2) and filled up to a final volume of 20 µl with nuclease-free water. Samples were placed in a Biometra T-Gradient thermocycler (Analytik Jena GmbH, Jena, Germany) and amplified (initial denaturation: 98°C, 30 s; denaturation: 98°C, 10 s, 30×; annealing/extension: 72°C, 50 s, 30×; final extension: 72°C, 15 s). Following amplification, PCR products were mixed with 10 µl 6× DNA Gel Loading Dye (Thermo Fisher Scientific, Waltham, MA, USA) and purified by electrophoresis on 1% agarose gels. Prior to Gibson assembly, the pAAVS1-Puro-DNR plasmid was linearized by double digest with EcoR1/Not1 restriction enzymes (New England Biolabs, Ipswich, MA, USA); 1 µg plasmid was mixed with 10× NEBuffer r3.1, 1 µl (20 units) EcoR1, and 1 µl (10 units) Not1 and filled up to 50 µl with nuclease-free water. The mixture was incubated for 15 min at 37°C and then purified on a 1% agarose gel. For the assembly, 100 ng linearized pAAVS1-Puro-DNR plasmid and 0.5 pmol of each of the two fragments were mixed with 10 µl 2× Gibson Assembly Master Mix (New England Biolabs, Ipswich, MA, USA) and filled up to 20 µl with nuclease-free water. The mixture was incubated at 50°C for 1 h and then stored at −20°C. For transfection, HEK 293 cells or Jurkat cells were seeded on a 6-well cell culture plate in 2 ml growth medium at a density of 3.5×10^5 cells/well and propagated over 24 h to a confluency of 50–70%. Prior to transfection, the medium was replaced with 900 µl fresh growth medium. For each well, 1 µg of donor DNA (pAAVS1-mCherry(NLS)-P2A-XIAP) and 1 µg of guide RNA (pCas-Guide-AAVS1) vectors were diluted with 250 µl Opti-MEM™, to which 2 µl (1 µl/µg DNA) PLUS™ Reagent was added. After 5 min, 6 ml Lipofectamine LTX was added and the mixture incubated for 20 min at room temperature, before being added dropwise to the corresponding wells. Cells were incubated for 72 h post transfection or until they reached 100% confluency and split 1:10. Puromycin (3 µg/ml) was added to the growth medium as selection antibiotic, and the cells were cultivated for 2 weeks, with medium replacement every 3–4 days. The surviving polyclonal cells were sorted for the highest mCherry fluorescence on a FACSMelody™ flow cytometer (Beckton-Dickinson, Franklin Lakes, NJ, USA). The obtained sub-population was singularized through dilution (20 cells/ml) in medium containing puromycin (3 µg/ml) and expanded on 96-well cell culture plates (100 µl/well ≈ 2 cells/well). To evaluate target expression, XIAP mRNA expression of the brightest clones was quantified by RT-PCR.

2.5 | Real-time quantitative polymerase chain reaction

Stable Jurkat XIAP and HEK XIAP cell lines, 2×10^6–4×10^7 cells were harvested and pelleted by centrifugation (5 min, 200 × g). The total RNA was extracted using the QIAShredder and RNeasy Plus Mini kit according to the manufacturer's instructions. RNA was eluted in nuclease-free water. The extracted RNA was quantified on a NanoDrop spectrophotometer using its absorption at 260 nm and stored at −80°C. For qPCR measurements, 1 µg total RNA was reverse-transcribed using the iScript™ cDNA synthesis kit according to the manufacturer's instructions. The resulting cDNA was either directly used or stored at −20°C. For each well of a 96-well qPCR plate, 2.5 ng cDNA were mixed with 10 µl 2× Fast SYBR Green RT-qPCR Master Mix (Thermo Fisher Scientific) and 250 nM of forward and reverse primers (for sequences see Table S2) and filled up to a final volume of 20 µl with nuclease-free water. The plate was sealed and placed in an iQ5 real-time PCR detection system (Bio-Rad, Hercules, CA, USA). Samples were amplified (polymerase activation: 95°C, 45 s; denaturation: 95°C, 10 s, 40×; annealing/extension: 60°C, 30 s, 40×; final extension: 60°C, 30 s). Following amplification, a melting curve analysis was performed to assess product homogeneity. Relative expression levels were calculated by the ΔΔCq method using GAPDH as reference gene and compared against vehicle treated or wild-type (WT) cells. Absolute expression levels of XIAP mRNA were determined using a calibration curve of synthetic XIAP amplicon (see Table S3; 1:10 dilution series, 10^{-13} to 10^{-21} mol). Statistical analysis (analysis of variance [ANOVA] with post hoc Tukey's test) was performed on ΔΔCq values with GraphPad Prism (GraphPad Software, San Diego, CA, USA).

2.6 | Cell delivery by electroporation

Electroporations were performed at room temperature or 4°C, using a Gene Pulser® Xcell™ electroporation system. Freshly harvested HEK-WT or HEK-XIAP cells were washed with PBS, spun down (5 min, 200 × g) and resuspended in room temperature or 4°C Gene Pulser® electroporation buffer at a concentration of 5×10^6 cells/ml. For each electroporation, 200 µl (800 µl) cell suspension was introduced in a room temperature or pre-chilled 0.2 cm (0.4 cm) gap size electroporation cuvette (Bio-Rad, Hercules, CA, USA), and the appropriate volume of PNA conjugate was added. After a quick resuspension, a single exponential decay pulse (routine electroporation: 0.55 kV/cm, 975°µF) was applied. Immediately after the pulse, 1.6 ml warm (37°C) recovery medium (DMEM + 20% [v/v] FCS, no antibiotics) was added and the cuvette placed in an incubator at 37°C and 5% CO_2. After 20 min, the cell suspension was taken up in 15 ml PBS and centrifuged (5 min, 200 × g). To screen for the optimal electroporation conditions, HEK-WT cells were electroporated with labeled PNA scr_biot. After recovery, cells were washed with 15 ml PBS (3×) and split 1:4 before being spun

down (5 min, 200 × g). The smaller pellet (ca. 2.5 × 10^5 cells) was resuspended in 1.25 ml growth medium and seeded on a 96-well plate at a density of 2 × 10^4 cells/well. The plate was incubated at 37°C and 5°% CO_2 for 24 h. Cell viability was determined by alamarBlue™ assay. The bigger pellet (ca. 7.5 × 10^5 cells) was resuspended in 750 µl PBS (theoretical concentration: 1.000 cells/ml). A solution of propidium iodide in PBS was added (final concentration: 1 µg/ml) and after 1 min incubation, cells were analyzed by flow cytometry (FAM = transfection efficiency: λ_{Ex} = 488 nm, λ_{Em} = 700 nm; PI = viability: λ_{Ex} = 561 nm, λ_{Em} = 613 nm). 30.000–50,000 events were recorded for each sample.

2.7 | Cell viability assay

To assess cell viability, the resazurin-based alamarBlue™ cell viability reagent was used. After treatment, cells were washed with 100 µl PBS and 100 µl of a 10% alamarBlue™ solution in PBS was added to each well. Plates were incubated for 1.5–2 h at 37°C and the fluorescence intensity was measured on a plate reader (λ_{Ex} = 530 nm and λ_{Em} = 590 nm). After subtraction of a blank, the fluorescence intensity relative to an untreated control was plotted and the graph fitted using a non-linear regression. IC_{50} values were determined from the resulting dose–response curves, as the concentration that produced half-maximal response.

2.8 | Flow cytometric apoptosis assay

After treatment, the medium containing dead cells and cell debris was removed from the wells and stored in a microcentrifuge tube. Cells were washed with 1 ml PBS, and the washing solution was likewise added to the microcentrifuge tube. Cells were detached with Trypsin–EDTA solution (0.25%) for 3–5 min at 37°C and taken up in the medium from the microcentrifuge tube. Cells were spun down (5 min, 200 × g) and washed with PBS (1×) before being stained. Flow cytometric Caspase-3/7 assays were performed with the CellEvent™ Caspase-3/7 Green Ready Flow™ Reagent. Dead cells were stained with SYTOX™ AADvanced™ Dead Cell Stain. Washed cells were taken up in 200 µl PBS with 0.5% BSA (w/v); 16.5 µl CellEvent™ Caspase-3/7 Green Ready Flow™ Reagent (2 drops or 82 µl per 1 ml cell suspension; 1 × 10^6 cells/ml) was added, and the cells incubated for 30 min at 37°C and 5% CO_2; 16.5 µl (2 drops or 82 µl per 1 ml cell suspension; 1 × 10^6 cells/ml) SYTOX™ AADvanced™ dead cell stain was added, and the cells stored on ice until analysis. Flow cytometric Annexin V assays were performed with Annexin V Alexa Fluor™ 488 conjugate. Dead cells were stained with SYTOX™ AADvanced™ Dead Cell Stain; 1× Annexin Binding Buffer was prepared by diluting 5× Buffer (50 mM HEPES, 700 mM NaCl, 12.5 mM $CaCl_2$, pH 7.4) 1:5 with ultrapure water. Washed cells were taken up in 200 µl 1× Annexin Binding Buffer; 5 µl Annexin V Alexa Fluor™ 488 conjugate (5 µl per 100 µl cell suspension; ~1 × 10^6 cells/ml) was added, and the cells incubated for 15 min at room temperature; 16.5 µl (2 drops or 82 µl per 1 ml cell suspension; 1 × 10^6 cells/ml) SYTOX™ AADvanced™ dead cell stain was added, and the cell suspension stored on ice until analysis. Cells were analyzed using filter set A (λ_{Ex} = 488 nm, λ_{Em} = 700 nm; SYTOX™ AADvanced™ dead cell stain), filter set B (λ_{Ex} = 488 nm, λ_{Em} = 527 nm; CellEvent™ Caspase-3/7 stain), and filter set C (λ_{Ex} = 561 nm, λ_{Em} = 613 nm; mCherry). Cells were divided in three populations: alive (CellEvent™/ SYTOX™ negative), apoptotic (CellEvent™ positive/SYTOX™ negative) and dead (SYTOX™ positive). For gating strategy see Figure S3; 30 000–50 000 events were recorded for each sample.

2.9 | Treatment of cells with reactive PNA conjugates

Cells electroporated with N_3-SMC and Ru(II)-PNA conjugates were resuspended in 1 ml Fluoro-Brite™ DMEM (theoretical concentration: 1000 cells/ml); 500 µl (approximately 500 000 cells) was transferred to 8 wells each of two 48-well cell culture plates. One plate was placed on a custom-built microplate heater set to 37°C and irradiated (λ = 455 nm) for 30 min using an M455L3-C1 LED lamp mounted 15 cm above. The lamp was controlled by a DC2200 LED driver (Thorlabs, Newton, NJ, USA) and operated at a current limit of 1000 mA and an intensity of 98%. The other plate was incubated 30 min at 37°C in the dark. After incubation, 500 µl DMEM supplemented with 20% (v/v) FCS and 2% (v/v) Penicillin/Streptomycin mixture (100 U/ml) was added to each well; 180 µl (approximately 100 000) and the cell suspension was transferred to a 96-well cell culture plate. The plates were placed in an incubator at 37°C and 5°% CO_2. After 1 h, 20 µl medium or a dilution of Super*Killer*TRAIL™ in medium (10 ng/ml; final concentration 0.5 ng/ml) was added, and the cells incubated for another 23 h. The next day, viability was evaluated by alamarBlue™ assay.

For alamarBlue™ viability assays with cells that were electroporated with N_3-SMC- and dmTCEP-PNA conjugates, cells were resuspended in 2.4 ml normal growth medium; 150 µl (approximately 62 500 cells) was transferred to each well of a 96-well cell culture plate. The plates were placed in an incubator at 37°C and 5% CO_2. After 1 h, 10 µl medium or a dilution of Super*Killer*TRAIL™ in medium (8 ng/ml; final concentration 0.5 ng/ml) was added, and the cells incubated for another 23 h. The following day, viability was evaluated by alamarBlue™ assay. For flow cytometry-based apoptosis assays, cells electroporated with N_3-SMC- and dmTCEP-PNA conjugates were resuspended in 4 ml normal growth medium (theoretical concentration: 250 cells/µl); 1 ml (approximately 250 000 cells) was transferred to each well of a 12-well cell culture plate. The plates were placed in an incubator at 37°C and 5°% CO_2. After 1 h, 50 µl medium or a dilution of Super*Killer*TRAIL™ in medium (10.5 ng/ml; final concentration 0.5 ng/ml) was added, and the cells incubated for another 23 h. The following day, viability was evaluated by a flow cytometry-based apoptosis assay.

2.10 | Isolation of probes from electroporated cells

The cell suspensions of 2–4 electroporations in 0.4 cm cuvettes were combined (8–16 × 10^6 cells). After recovery, cells were washed with 15 ml PBS (3×) and optionally irradiated as described above. Cells were spun down (5 min, 200 × g) and lysed in 1 ml RIPA buffer (50 mM Tris, 150 mM NaCl, 1% Triton X-100, 0.1% (w/v) SDS, 1 mM EDTA, pH 7.4, 1 cOmplete™ Mini protease inhibitor tablet per 10 ml) on ice for 20 min with intermittent sonication every 5 min (3 s, duty cycle: constant, output: 7; Sonifier 450, Branson Ultrasonics, Danbury, CT, USA). Cellular debris was removed by centrifugation (16 900 × g, 10 min, 4°C); 50 µl magnetic streptavidin beads Dynabeads® M-280 (binding capacity: 100 pmol; Thermo Fisher Scientific Waltham, MA, USA) were washed with 500 µl RIPA buffer (3×) and added to the samples. The mixture was incubated overnight at 4°C with constant rotation. The next day, the supernatant was removed, and the beads were washed with TBS-T (10 mM Tris, 150 mM NaCl, 0.05% (v/v) Tween-20, pH 7.4). Biotinylated peptides were eluted by suspending the beads in 25 µl of an aqueous 70% (v/v) MeCN, 5% (v/v) formic acid, 1 mM biotin solution, and incubating then at 37°C for 2 h. The eluted peptides in the supernatant were analyzed by fluorescence-monitored UPLC (system B, column 4; see Table S4 for details).

2.11 | Templated reactions in total RNA isolate

To prepare total RNA isolate, 2 × 10^8 HEK-WT or HEK-XIAP cells were harvested and pelleted by centrifugation (5 min, 500 × g). Total RNA was isolated with TRIzol™ reagent (Thermo Fisher Scientific, Waltham, MA, USA) according to the manufacturer's instructions: 10 ml TRIzol™ reagent was added to the pellets and the mixture homogenized by pipetting up and down (5 min); 2 ml chloroform (0.2 ml per 1 ml TRIzol™ used) were added, and the samples mixed by inversion. After 2 min incubation on ice, the samples were centrifuged (15 min, 12 000 × g, 4°C), and the colorless upper aqueous phase transferred to a new tube; 5 ml isopropanol (0.5 ml per 1 ml TRIzol™ used) were added, and the mixture incubated at −18°C for 1 h. The resulting precipitate was collected by centrifugation (10 min, 12 000 × g, 4°C), and the supernatant removed with a pipette. The pellet was washed by vortexing it for 1 min in 10 ml cold 75% (v/v) ethanol (1 ml per 1 ml TRIzol™ used) and centrifugation (5 min, 7.500 × g, 4°C). After removing the supernatant, the pellet was air dried (approximately 10 min) and re-dissolved in 200 µl (1 µl per 1 × 10^6 cells) buffer (10 mM MOPS, 200 mM NaCl, 0.1% [w/v] CHAPS, pH 7.0) by gentle shaking and intermittent heating in a 40°C water bath. For templated Staudinger reductions, 50 µl total RNA isolate was placed in low-binding micro tubes (Sarstedt, Nümbrecht, Germany) and warmed to 37°C on a thermoshaker. After addition of 5 mM sodium ascorbate fluorescein- and biotin-labeled N_3-SMC-PNA (2 µM), RNA template (1 eq. if added) and Ru(II)-PNA (4 µM) were added, and the mixture was irradiated (λ = 455 nm) at 37°C for 60 min. The samples were diluted 1:20 with RIPA buffer (50 mM Tris, 150 mM NaCl, 1% Triton X-100, 0.1% [w/v] SDS, 1 mM EDTA, pH 7.4, 1 cOmplete™ Mini protease inhibitor tablet per 10 ml); 50 µl magnetic streptavidin beads Dynabeads® M 280 (binding capacity: 100 pmol; Thermo Fisher Scientific, Waltham, MA, USA) were washed with 500 µl RIPA buffer (3×) and added to the samples. The mixture was incubated overnight at 4°C with constant rotation. The next day, the supernatant was removed, and the beads were washed with TBS-T (10 mM Tris, 150 mM NaCl, 0.05% [v/v] Tween-20, pH 7.4). Biotinylated peptides were eluted by suspending the beads in 25 µl of an aqueous 70% (v/v) MeCN, 5% formic acid, 1 mM biotin, and incubating then at 37°C for 2 h. The supernatant was analyzed by RP-UPLC as described in Section 2.10.

3 | RESULTS AND DISCUSSION

3.1 | Design of a nucleic acid templated reaction leading to activation of an SMC

SMCs such as BV6[56] (Figure 3A) confer a pro-apoptotic effect by binding to the BIR2 and BIR3 domains of the XIAP, which can then no longer block caspase-9.[57,58] In addition, SMCs also bind cIAP-1 and -2 and induce their ubiquitylation causing degradation by the proteasome.[56,59,60] Both proteins counteract the activation of the extrinsic apoptosis pathway by inducing the expression of anti-apoptotic genes upon signaling through the tumor necrosis factor receptor 1 (TNFR1). As a result, SMC treatment restores a cell's ability to respond to apoptotic stimuli.

The activity of most SMCs depends on their *N*-terminal amino group, which forms multiple hydrogen bridges with the BIR domain binding pocket.[52] Modifications such as dimethylation or acetylation that prevent protonation are detrimental for binding.[52,61] We have

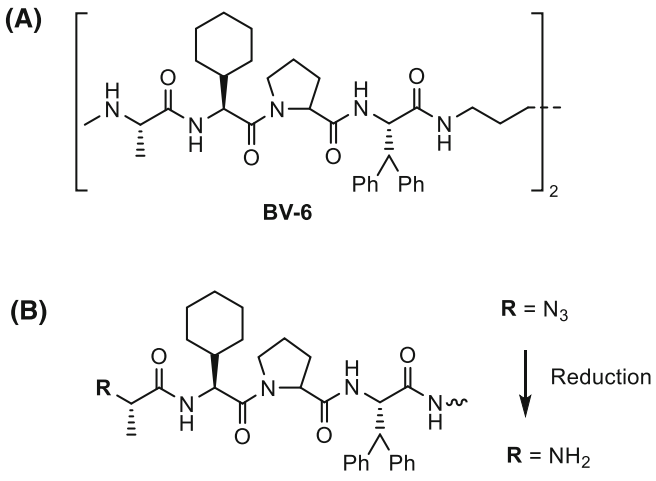

FIGURE 3 (A) The peptidomimetic BV6 antagonizes inhibitor of apoptosis proteins XIAP, cIAP-1, and cIAP-2. BV6 binds baculovirus IAP repeat (BIR) domains 2 and 3 of XIAP with nanomolar affinity. (B) An *N*-terminally azido-modified derivative of MV1 reduces XIAP affinity by three orders of magnitude. Reduction of the azido group restores XIAP affinity.[48]

shown that the replacement of the *N*-terminal amine of MV1, the monovalent version of BV6, by an azido group reduces the affinity by three orders of magnitude (Figure 3B).[48] For an RNA-templated reaction, which restores the pro-apoptotic activity of an azido-inactivated SMC, we had considered two types of templated reactions acting on N_3-SMC-PNA (**N3**): Staudinger reduction with a PNA-linked phosphine and a photocatalyzed reduction using a Ru(II)-complex attached to PNA (Figure 4). Both reactions have previously been employed for the RNA-templated reduction of dye azides.[20,42]

To explore templated unmasking of an N_3-SMC, we prepared PNA conjugates that would bind mRNA templates encoding for XIAP. This way, overexpression of XIAP mRNA in tumor cells would trigger the formation of a SMC antagonizing the overexpressed protein. XIAP mRNA has recently been targeted by antisense molecules.[62] As an N_3-SMC, we used the MeAla-Chg-Pro-Dip tetrapeptide also known as MV1.[56] For the synthesis of a conjugate, a lysine residue at the *N*-terminus of PNA was extended via the side chain during solid phase synthesis. For the synthesis of the PNA-linked reducing agents, PNA was prepared with an Alloc-side chain protected lysine residue at the *C*-terminus, which, after deallylation, was used for on-resin coupling of dimethyl protected TCEP. A similar approach was used for the introduction of the $Ru(bpy)_2(mcpy)$ complex.

3.2 | Templated reduction of azido-SMC-PNA in vitro

Prior to experiments in cells, the two templated N_3-SMC reduction reactions were analyzed by UPLC analysis. Two equivalents of the reducing conjugate were combined with one equivalent of N3 and RNA template. At 37°C, the Staudinger reaction proceeded quickly and provided 60% yield of H_2N-SMC-PNA in only 15 min (Figure 5A).

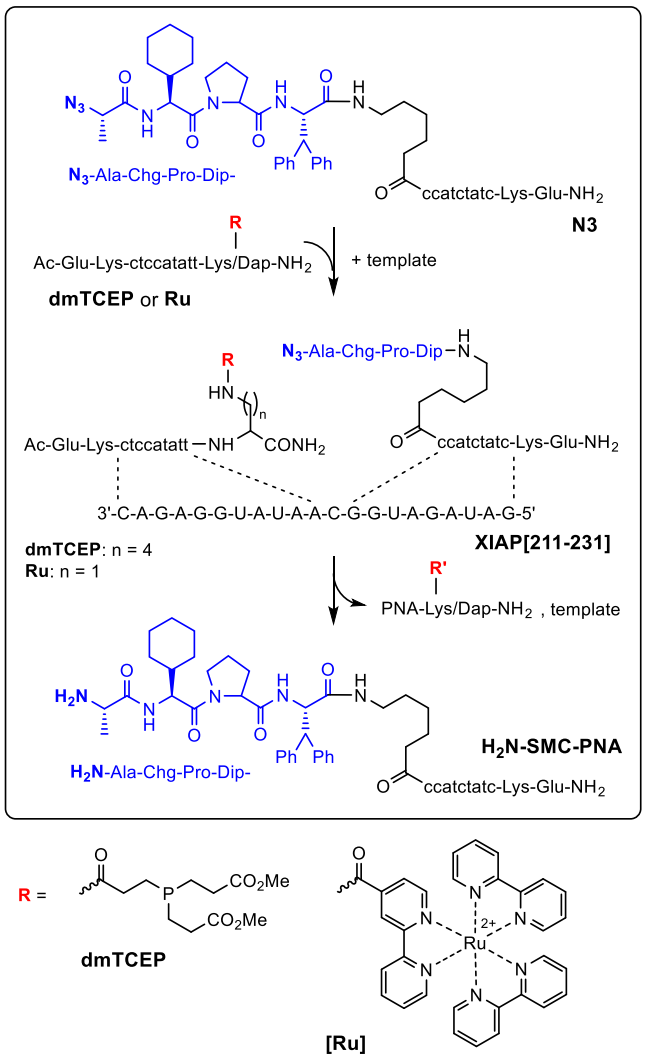

FIGURE 4 RNA-templated reduction of azido-Smac mimetic peptide-PNA conjugate N3 with phosphine-armed peptide nucleic acid (PNA) dmTCEP or $Ru(bpy)_2(mcbpy)$-modified PNA Ru

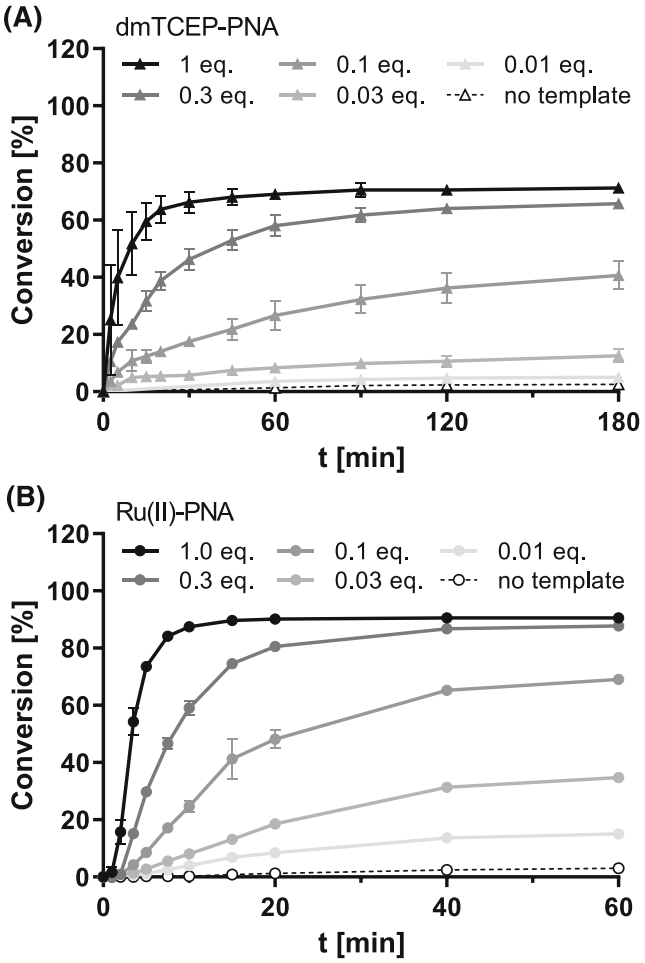

FIGURE 5 Templated reduction of N3 in (A) Staudinger reaction with phosphine-peptide nucleic acid (PNA) dmTCEP or (B) photocatalytic reduction with ruthenium-PNA Ru at varying amounts of RNA template XIAP[211–231]. Conditions: (A) 1 μM N3, 2 μM dmTCEP in buffer (10 mM MOPS, 200 mM NaCl, 0.1% CHAPS, pH 7.0), 37°C. (B) 1 μM N3, 2 μM Ru in buffer (10 mM MOPS, 200 mM NaCl, 0.1% CHAPS, 5 mM NaAsc, pH 7.0), 37°C, irradiation with 0.98 W LED, λ = 455 nm

The reaction reached a plateau at 70% after 60 min. Without template, product formation was negligible. Next, we assessed the reaction on substoichiometric amounts of template. On 0.1 eq template, the reaction afforded 40% yield. Given the 1 μM concentration of N3 involved, this corresponds to 400 nM product. Of note, 30 nM concentration of template (0.03 eq) induced the formation of 100 nM product.

For an evaluation of the Ru(II)-based probe Ru, the experimental setup was slightly modified. Instead of micro reaction tubes, the reactions were performed in black, low-binding multiwell plates under a collimated LED light source (1 W, $\lambda = 455$ nm). The Ru(II)-PNA-catalyzed reactions proceeded significantly faster than the Staudinger reactions. Using equimolar amounts of RNA template, up to 90% H_2N-SMC-PNA was formed within in 15–20 min. Again, background in absence of template was extremely low. When the amount of template was decreased, it became apparent that the [Ru]-based reduction is catalytically more active than the Staudinger reduction. In the presence of 0.03 eq. template (30 nM), the Ru probe provided 40% yield after 60 min, as opposed to only 10% in the Staudinger reduction. Most noteworthy was the reaction on 0.01 eq template. Under these conditions, the Staudinger reduction was inefficient. By contrast, 10 nM template instructed the formation of 150 nM product when Ru was used. The different catalytic efficiencies are due to differences of the reaction mechanism. The Staudinger reduction depletes the concentration of both the N_3-SMC-PNA and the reducing agent dmTCEP-PNA. Therefore, two strand exchange reactions are necessary to enable turnover. Only a single strand exchange is sufficient for Ru, because the photoreductively active [Ru]-species is regenerated in presence of ascorbate as stoichiometric reductant. We concluded: Using a concentration of 1 μM N_3-SMC-PNA (N3), significant amounts of product H_2N-SMC-PNA could be formed with only 10 nM template, a concentration that may realistically be achieved in overexpressing cells.

3.3 | Creation and evaluation of a cell line overexpressing a XIAP mRNA segment

Next, we constructed a cell line that overexpresses XIAP mRNA. To maintain responsiveness to apoptotic stimuli, we designed a short, non-functional XIAP mRNA fragment (coding for aa 43–109) containing the target sequence. This gene fragment was inserted into a pAAVS1 donor vector via Gibson assembly (for plasmid map, see Supporting Information). The resulting fusion sequence mCherry(NLS)-P2A-XIAP was put under the strong human cytomegalovirus (CMV) promotor to ensure high expression levels. The construct contains a P2A self-cleaving peptide sequence, which separates the nuclear localization sequence (NLS)-tagged fluorescent mCherry protein from the XIAP fragment upon translation. The former migrates to the nucleus and was used for evaluation of transfection efficiency and for flow cytometric sorting of the cells according to their expression level. The sorted cells were singularized, and individual clones expanded under puromycin selection.

Our initial attempts focused on transfection of a Jurkat cell line, which is susceptible to treatment with SMCs. To compare their relative XIAP mRNA expression levels, a RT-qPCR analysis with primers spanning the target sequence was conducted. The highest expressing clone, C10, was subjected to quantification of the target copies per cell, using a synthetic amplicon as reference (Figure 6). Unfortunately, C10 demonstrated an only 22-fold higher expression level than WT Jurkat cells. This corresponds to a copy number of approx. 490 molecules per cell. Given an average Jurkat cell volume of 0.66 pl,[63] this translates into an intracellular concentration of about 1 nM (50 pM for Jurkat WT), significantly below the previously established limit of the templated reaction. Assuming that most of the cellular mRNA resides in the cytoplasm after nuclear export (which comprises about one-third of the cellular volume), this value may be slightly higher (3 nM), but based on results from the turn-over experiments, this was considered still too low.

The weak expression was attributed to the inefficient transfection of Jurkat cells, a well-known problem of this cell line. As an alternative, a new attempt was made with easier-to-transfect HEK 293 human embryonic kidney cells. Although not a cancer cell line, HEK 293 cells are tumorigenic in nude mice and can be considered a model for malignant neoplasms. Like cancer cells, they have a severely deregulated transcriptome and overexpress certain cancer associated genes.[64] Control experiments revealed that HEK 293 cells respond to proaptotic stimuli set by the combined action of the enhanced TNF-based agent Super*Killer*TRAIL™ and an SMC such as BV6 (Figure S1). It was thus reasoned that XIAP-overexpressing HEK 293 cells may serve as an easier-to-handle model system for the templated reaction. Indeed, the modification of HEK 293 cells proved to be more successful, and several highly expressing clones were obtained (Figure S2). Out of five selected candidates, A5 had the best combination of overexpression and efficient growth. The absolute quantification of its XIAP mRNA levels by RT-qPCR revealed an increase over WT levels by more than 146-fold, to an absolute number of 14 200 molecules per cell (Figure 6). Assuming an average cell volume of 1.4 pl (calculated from

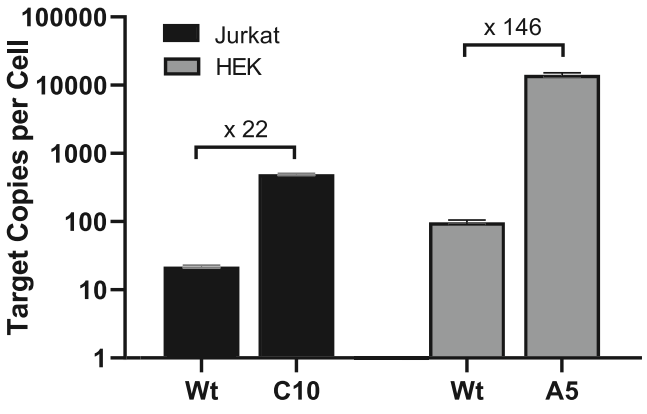

FIGURE 6 Evaluation of target mRNA expression levels in engineered cell lines. Comparison of absolute X-linked inhibitor of apoptosis protein (XIAP) mRNA expression levels in Jurkat wild-type (WT) cells and HEK 293 cells and clones stably expressing the target gene

the average diameter of HEK 293 WT cells of 13.9 µm[65] and assuming spherical shape), this corresponds to an intracellular target mRNA concentration of approximately 17 nM (115 pM for HEK WT).

3.4 | Cellular delivery of PNA conjugates

Lipofection is a convenient and efficient approach for delivery of oligonucleotides into cells. Unfortunately, PNA cannot be lipofected. A frequently used delivery method takes advantage of cell penetrating peptides (CPPs).[66] However, previous research from our group exposed the high cytotoxicity of conjugates combining an SMC agent, a PNA unit, and a CPP module.[54] We, therefore, decided to employ electroporation for delivery. To screen for suitable pulse settings, HEK cells were suspended in electroporation buffer at a concentration of 5×10^6 cells/ml. A carboxyfluorescein-labeled PNA-probe (2 µM N_3-Ala-Chg-Pro-Dip-Ahx-accttacct-Lys(FAM)-Lys(Biotin)-Glu-NH_2, scr_biot) was added to the suspension to allow a quantification of the uptake by flow cytometry. Varying the voltage of an exponential decay pulse with a capacitance of 975 µF, it was learned that efficient delivery (>80% positive cells) occurs at field strengths above 0.55 kV/cm (Figure 7A). However, post-pulse cell viability, assessed after 4 h by propidium iodide staining (flow cytometry) or after 24 h by alamarBlue™ assay, was negatively correlated with increasing voltage. Only about 60% of the electroporated cells remained viable 4 h after a 110 V pulse, and of these, half died within the next 24 h. Electroporating the cells in ice-cold buffer using pre-chilled electroporation cuvettes and recovering them in warm (37°C) medium supplemented with 20% serum immediately after the pulse significantly enhanced viability without compromising transfection efficiency (Figure 7B). Using this procedure at a voltage of 110 V, more than 80% of the cells survived, and around 45% were still viable the next day. These conditions were selected for the delivery of the reactive probes.

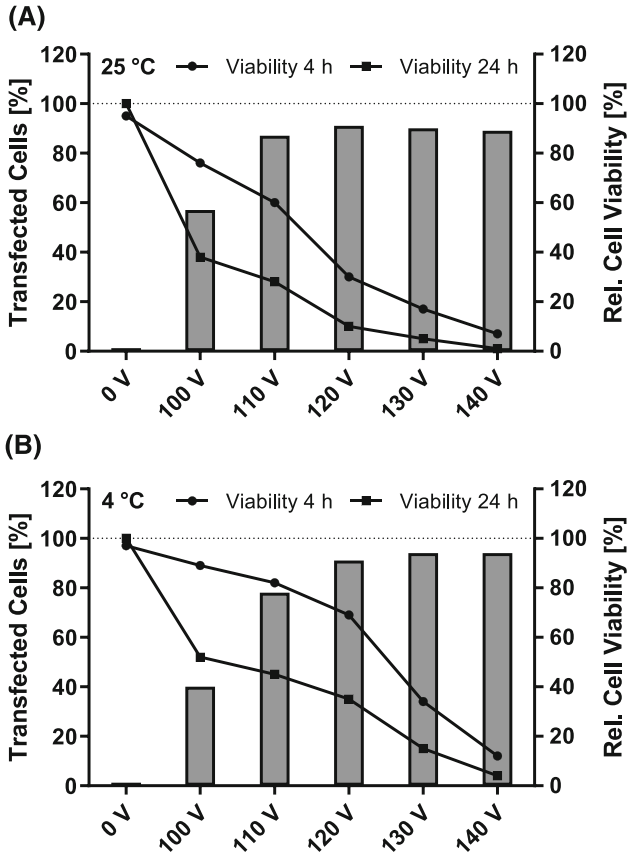

FIGURE 7 Optimization of electroporation conditions. HEK 293 cells were suspended in (A) 25°C or (B) 4°C GenePulser buffer (5×10^6 cells/ml) containing 2 µM N_3-Ala-Chg-Pro-Dip-Ahx-accttacct-Lys(FAM)-Lys(Biotin)-Glu-NH_2 (scr_biot) and electroporated using tempered 0.2 cm cuvettes and a single exponential decay pulse at 975 µF with varying voltage. Transfection efficiency was assessed after 4 h by flow cytometry as the ratio of FAM-positive to negative cells. Viability was determined after 4 h by propidium iodide staining (FACS) or after 24 h by alamarBlue™ assay.

3.5 | Exploring templated photocatalytic reaction with azido-SMC-PNA in target-overexpressing HEK 293 cells

The evaluation of the templated reduction of N_3-SMCs in cells was commenced with Ru(II)-PNA probe Ru, which in test tubes provided a higher reactivity than the phosphine-based Staudinger probe dmTCEP. For each experiment, HEK XIAP A5 and WT cells were electroporated with combinations of Ru(II)-PNA (Ru) and match (N3) or scrambled (scr) N_3-SMC-PNA probes using the optimized electroporation conditions. To provide sufficiently high intracellular concentrations, up to 10 µM of the N_3-SMC-PNA conjugate was added to the electroporation buffer. Due to its catalytic activity, a smaller amount (up to 2 µM) of the Ru(II) conjugate Ru was used. To avoid toxic effects caused by irradiation of cells at 455 nm, we used a proprietary DMEM-reformulation (FluoroBrite™), which has reduced concentration of phototoxic components. Ru(II)-PNA (Ru) and N_3-SMC-PNA (N3) were co-electroporated and, after a 20 min recovery phase, irradiated for 30 min. Cell viability was evaluated in an alamarBlue™ assay after 24 h. Compared with incubation of cells with Ru and N3 in the dark, irradiation reduced cell viability by more than 40% (Figure 8A). After 1 h of irradiation, cells were treated with the enhanced TNF derivative Super*Killer*TRAIL™. This reduced viability in a dose-dependent fashion. Compared with experiments with the N_3-SMC-PNA conjugate N3, the co-electroporation of N3 and Ru was significantly more potent in reducing viability. However, control experiments revealed that this effect was also achieved with the ruthenium probe Ru alone. In an additional set of experiments, we varied the concentration of the Ru-probe Ru while keeping the concentrations of matched (N3) and a scrambled (scr) N_3-SMC-PNA constant. The viability decrease caused by irradiation was positively correlated with the concentration of Ru, which proved phototoxic over a wide concentration range (Figure 8B). Moreover, no difference

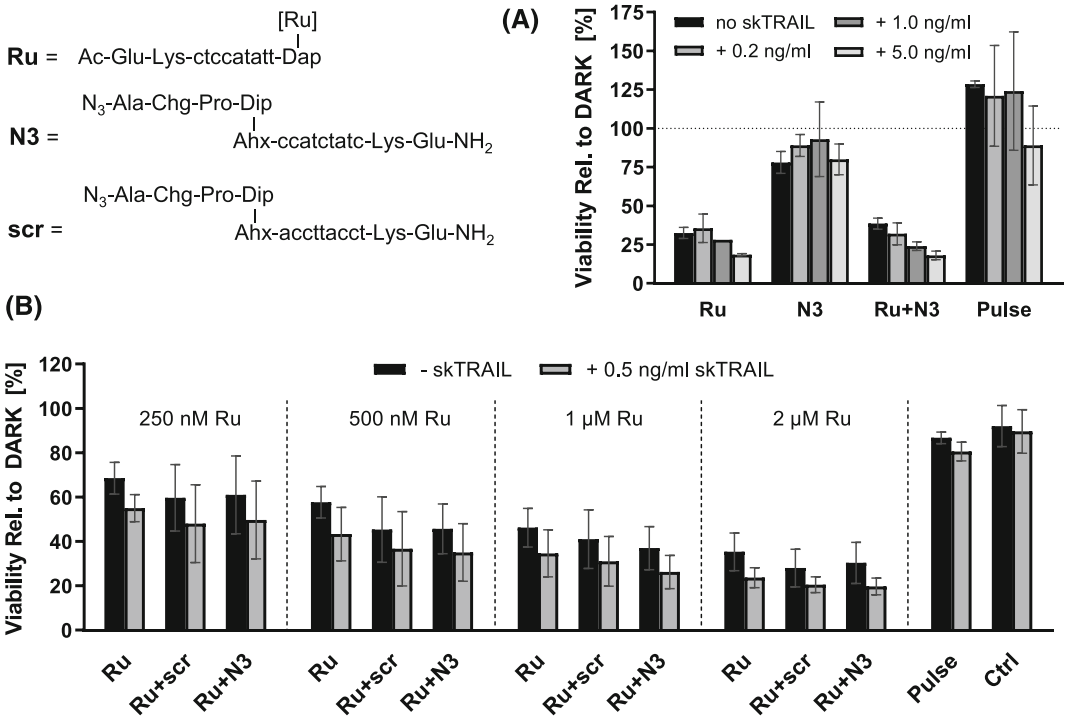

FIGURE 8 Viability of HEK XIAP A5 cells 24 h after electroporation and irradiation with combinations of (A) 10 µM N_3-SMC-PNA (N3) and 1 µM Ru(II)-PNA (Ru) in presence or absence of 0–5 ng/ml Super*Killer*TRAIL™ or (B) combinations of 5 µM match (N3) or scrambled (**scr**) N_3-SMC-PNA and 0.25–2 µM Ru(II)-PNA (Ru) in the presence or absence of 0.5 ng/ml Super*Killer*TRAIL™, relative to a corresponding non-irradiated (DARK) control

could be detected between cells that had been treated with Ru and match conjugate N_3-SMC-PNA (N3), or those that received the scrambled control N_3-SMC-scrPNA (scr), indicating that any detectable differences to the Ru-only treated sample were likely not due to a templated reaction taking place. The addition of death ligand Super*Killer*TRAIL™ reduced the overall cell viability but failed to produce a specifically higher toxicity of the reaction system.

It was conceivable that the yield of the templated reaction was not sufficient to produce a viability drop large enough to be detected by the assay. To determine whether a reaction is taking place in the cells at all, a set of analogous biotin- and carboxyfluorescein-labeled NH_2/N_3-SMC-PNA probes for product isolation and detection was prepared (N3_biot and scr_biot, Figure 9). The templated photocatalytic reduction of the FAM-N_3-SMC-PNA (N3_biot) was analyzed by UPLC. Again, in test tubes, the templated reaction proceeded smoothly (Figure 9A), showing that conjugation of the N_3-SMC-PNA with biotin and FAM is not perturbing. To isolate the potential product of an intracellular templated reaction, HEK XIAP A5 and HEK WT cells were electroporated with Ru(II)-PNA (Ru) and match (N3_biot) or scrambled (scr_biot) biotin-/FAM-labeled N_3-SMC conjugate and irradiated for 30 min. Immediately after, the cells were lysed in RIPA buffer with protease inhibitors. Magnetic streptavidin-coated beads were used to isolate all biotin-bearing compounds. However, the subsequent analysis on a UPLC instrument equipped with a fluorescence detector did not reveal any significant product formation (Figure 9B). Although a very small peak with the same retention time as the NH_2-SMC-PNA reference conjugate H_2N_biot (3.1 min) was present in all samples, samples isolated from WT cells gave identical chromatograms, indicating the absence of a catalytic effect by overexpressed XIAP mRNA. To address the question whether the cellular mRNA could catalyze a reaction in a less complex environment (i.e., in the absence of non-nucleic acid components and cellular compartmentalization), total RNA was isolated from both HEK XIAP and HEK WT cells and re-dissolved at physiological concentration in buffer (10 mM MOPS, 100 mM NaCl, 0.1% CHAPS, pH 7.0; 1 pl/cell lysed). The reactive probes (N3_biot and Ru) were added, and the mixtures were irradiated for 60 min. Subsequently, streptavidin bead extraction was performed. Like in the previous experiment, no product formation beyond background reaction could be detected in either HEK XIAP or WT RNA isolate (Figure 9C). To verify the reactivity of the probes, RNA extract was spiked with an additional 1 µM synthetic XIAP RNA. A nearly full conversion was observed.

To test whether the templated reaction could be carried out in a cellular environment when sufficient amounts of mRNA template are present, synthetic target was co-electroporated into the cells. Due to the abundance of nucleases in the cellular environment, a 2′OMe-stabilized RNA template (XIAP 2′OMe-RNA[208–232]) was used instead of regular RNA. Control experiments in test tubes were

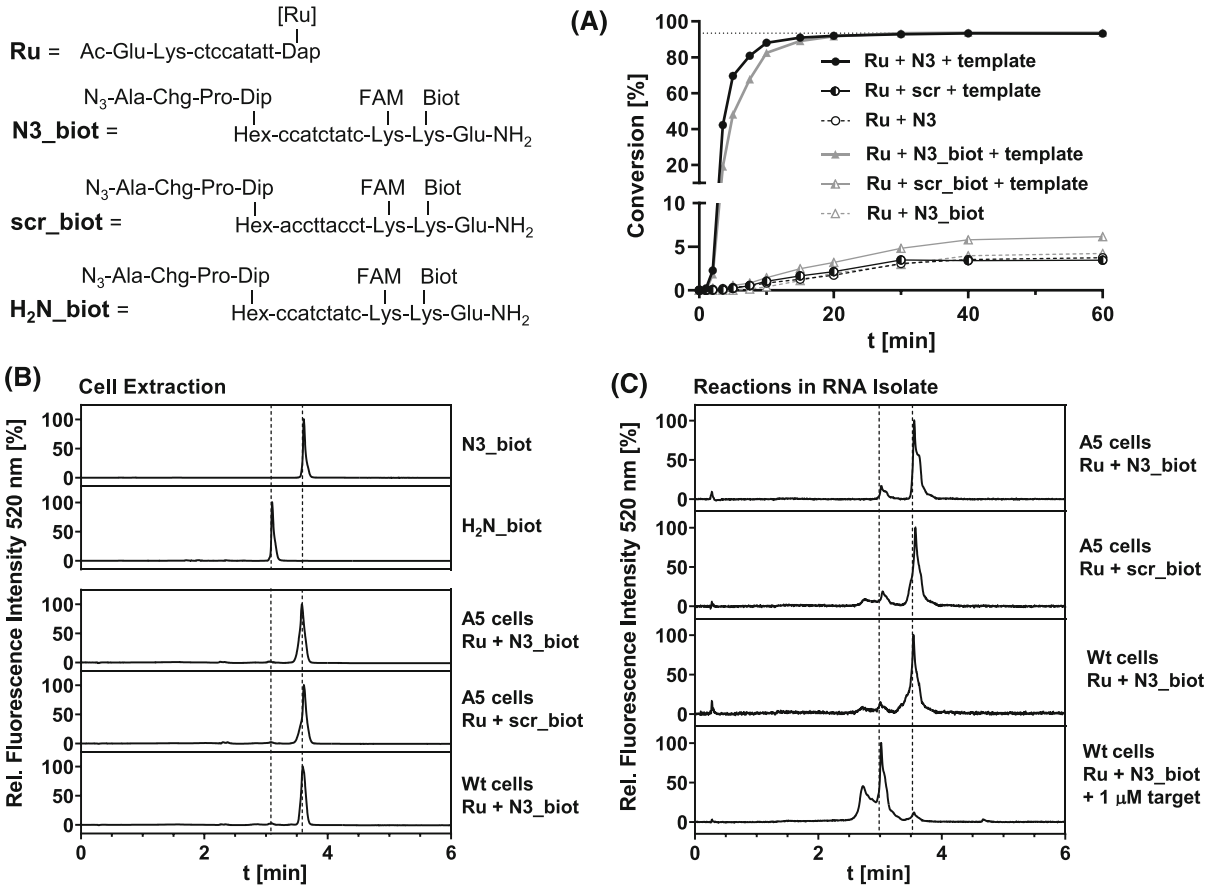

FIGURE 9 Evaluation of reactions in (A) test tubes, (B) cells, and (C) RNA extract. Conditions: (A) 2 μM Ru, 1 μM N3, or N3_biot; 1 μM RNA template if added, in buffer (10 mM MOPS, 200 mM NaCl, 5 mM NaAsc, 0.1% CHAPS, pH 7.0), irradiation (LED, 0.98 W, λ = 455 nm), 37°C. (B) HEK XIAP A5 (A5) or HEK wild-type (WT) cells were electroporated with 5 μM authentic reference H_2N_biot or N3_biot or scrambled sequence control scr_biot with or without 1 μM Ru and irradiated for 30 min (0.98 W; λ = 455 nm). Streptavidin bead extracts of lysates were evaluated by FL-UPLC analysis (λ_{ex} = 495 nm, λ_{em} = 520 nm). (C) RNA isolates from HEK Wt cells or HEK A5 cells were re-dissolved at physiological concentration (1 pl/cell) in buffer (10 mM MOPS, 200 mM NaCl, 5 mM NaAsc, 0.1% CHAPS, pH 7.0), treated with 2 μM Ru, 1 μM N3_biot or scr_biot and XIAP RNA[211–231] template (if added) and irradiated for 60 min (0.98 W; λ = 455 nm) prior to analysis of streptavidin bead extracts by fluorescence-monitored ultra-high performance liquid chromatography (UPLC)

performed to verify that 2′-OMe template was able to promote the reduction of the N_3-SMC-PNA probe (Figure 10A). Using stoichiometric concentrations of 2′OMe-RNA (1 μM), 90% product were obtained in 15 min, the same kinetics as for reactions on the unmodified RNA template XIAP RNA[211–231]. At sub-stoichiometric concentrations (0.1 μM), the reaction was slower, yielding only 60% instead of 70% product within the 60 min timeframe of the experiment, which might be due to a higher melting temperature of the PNA:2′OMe-RNA duplex. Regardless, the 2′OMe-RNA template was used in a cell experiment (Figure 10B). The combination of Ru(II)-PNA (Ru), match N_3-SMC-PNA (N3), and template decreased the viability to 30% compared with 36% when N3 was lacking or replaced by a scrambled sequence. Considering the standard deviation, this is not significant. Furthermore, no product was found in a streptavidin bead extraction following co-transfection of 10 μM Ru, N3, and 2′OMe-RNA template (data not shown).

3.6 | Exploring templated Staudinger reduction of azido-SMC-PNA in target-overexpressing HEK 293 cells

We considered the possibility that the cellular reducing agents are ineffective at (re)generating the ruthenium catalyst. Therefore, we decided to explore the reactivity of electroporated probes that can trigger the Staudinger reduction, which does not depend on additional reducing agents.

The dmTCEP-PNA probe dmTCEP and N_3-SMC-PNA N3 were electroporated into the modified HEK 293 cells as described. Interestingly, a slightly stronger response to the combination of N3 and dmTCEP seemed to occur than to dmTCEP alone or the combination with scrambled N_3-SMC-PNA scr (Figure 11A). Although not statistically significant, the difference persisted over multiple repetitions of the experiment. It was decided to further investigate, using an

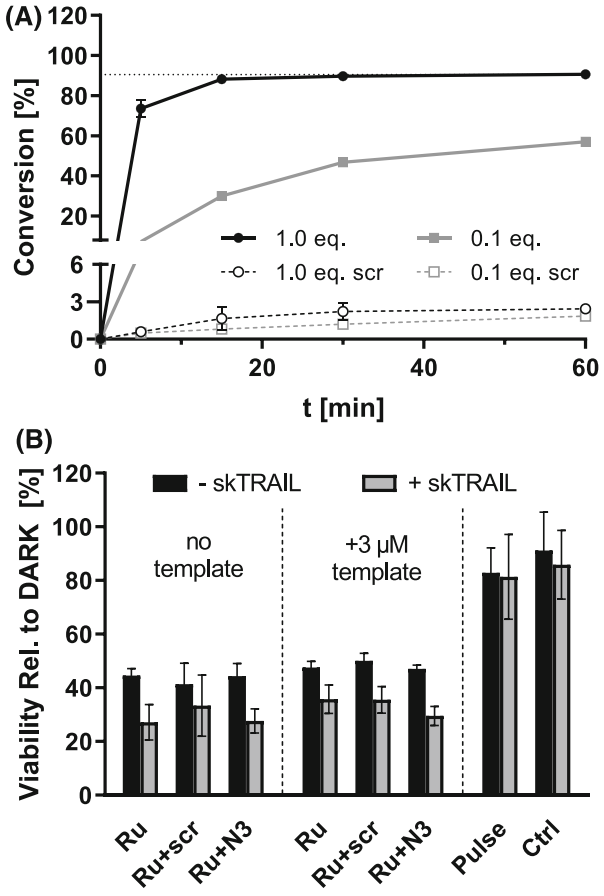

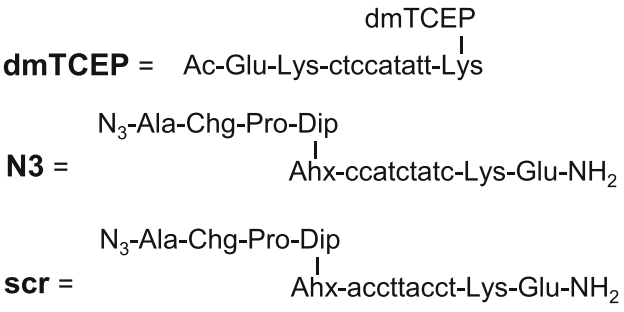

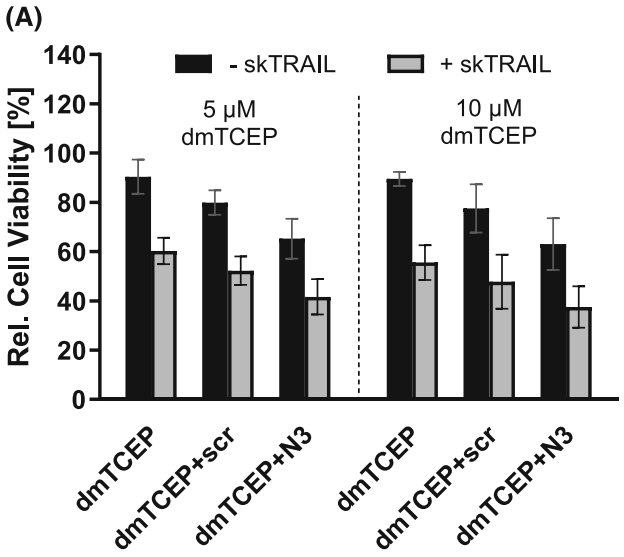

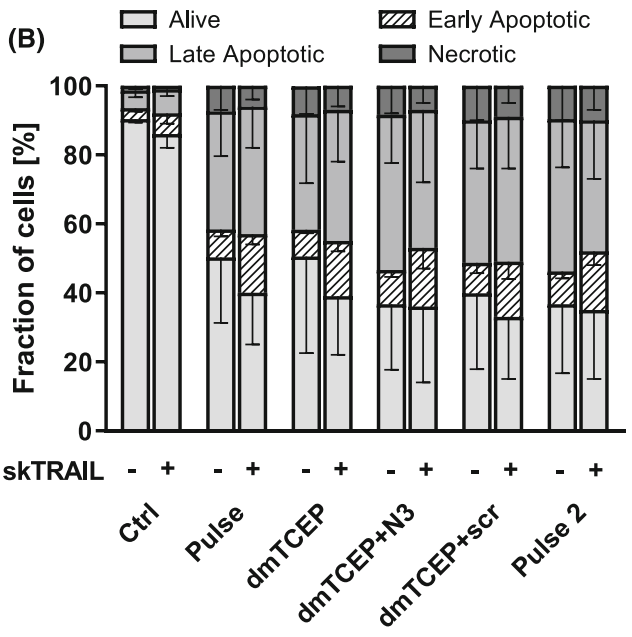

FIGURE 10 (A) Templated reaction between [Ru(II)]-PNA (Ru) and N3-SMC-PNA (N3) on synthetic 2′OMe RNA template (5′-GUAGAUAGAUGGCAAUAUGGAGACU-3′). Conditions: 2 µM Ru, 1 µM N3 and 1 µM template (if added) in buffer (10 mM MOPS, 200 mM NaCl, 5 mM NaAsc, 0.1% CHAPS, pH 7.0), 37°C, irradiation (LED, 0.98 W, λ = 455 nm). (B) Viability of HEK XIAP A5 cells electroporated with combinations of 5 µM match (N3) or scrambled (scr) N_3-SMC-PNA, 1 µM Ru(II)-PNA (Ru) and 0 or 3 µM XIAP 2′-OMe-RNA template [208–232] in presence or absence of 0.5 ng/ml Super*Killer*TRAIL™, relative to a non-irradiated (DARK) control.

Annexin-V and Caspase-3/7 flow cytometric apoptosis assay, respectively, which allow a finer discrimination between viable, dead, early, and late apoptotic cell populations. Annexin V is a phospholipid-binding protein that recognizes phosphatidylserine, which is presented by early apoptotic cells on their cell surface. For the assay, HEK XIAP A5 cells were electroporated with 5 µM match (N3) or scrambled (scr) N_3-SMC-PNA and 10 µM dmTCEP. After 24 h of incubation, the cell populations were marked with Annexin V-AlexaFluor488 or CellEvent Caspase-3/7 apoptosis detection reagent and a dead cell stain. When the relative shares of viable, apoptotic,

FIGURE 11 Legend on next page.

FIGURE 11 Treatment of HEK XIAP A5 cells with N_3-SMC- and dmTCEP-PNA conjugates. (A) Viability 24 h after electroporation with combinations of 5 μM match (N3) or scrambled (scr) N_3-SMC-PNA and 5/10 μM dmTCEP-PNA (dmTCEP) and incubation in the presence or absence of 0.5 ng/ml Super*Killer*TRAIL™, relative to a pulse-only control. Determined by alamarBlue assay. (B) Flow cytometric Annexin V-AlexFluor488/Sytox AADVanced apoptosis assay of cell populations 24 h after electroporation with combinations of 5 μM N3 or scr and 10 μM dmTCEP and incubation in presence or absence of 0.5 ng/ml Super*Killer*TRAIL™. Pulse-only controls were performed at different times after cells were incubated at 4°C: before (Pulse) and after (Pulse 2) other cells were electroporated.

and dead cell populations were plotted, the results were not drastically different from the previous viability assay (Figure 11B). Although the combined treatment with both dmTCEP and N3 appeared to produce a slightly larger proportion of late stage apoptotic and dead cells then dmTCEP alone, the difference between cells that received the match conjugate and those that were treated with the scrambled version remained insignificant. Like before, Super*Killer*TRAIL™ was added in an attempt to stimulate apoptosis, and although this treatment resulted in more apoptotic and fewer viable cells, it failed to amplify differences between treatments. Importantly, a second pulse-only control (Figure 11B; Pulse 2), which was performed last, after electroporation of all other samples, was included in this experiment. The fact that cells in this control were less viable than in the initial pulse-only control (Figure 11B; Pulse) hinted at a time dependency of cell viability. It suggested that samples that were electroporated later demonstrated lower viability in the assay. This was possibly a result of the different time the cells spent on ice during the procedure. Cold shock has been shown to induce apoptosis under certain conditions.[67] This effect might mask weak differences between the samples, and together with the relatively large error, this precludes statistically meaningful conclusions of the experiment.

4 | DISCUSSION

Although the templated reduction of N_3-SMCs proceeded sufficiently fast and very specific in a cell-free context (particularly the Ru(II)-catalyzed photoreduction), the approach could not be transferred into a cellular environment. The observed lack of a biological response specific to the reaction system could stem from multiple issues. The target sequence may be inaccessible to the conjugates. This could be the case if, for example, secondary or tertiary structure elements are present. Finding suitable annealing sites is a key issue in the development of effective antisense molecules. Although a truncated sequence XIAP mRNA sequence was chosen as target for the templated reaction, it cannot be excluded that the overexpressed mCherry(NLS)-XIAP RNA adopts a structure that hinders accessibility.

Another possibility is that the levels of template RNA in the cells might not suffice to catalyze the templated reaction to the necessary extent. RT-qPCR experiments revealed that HEK XIAP clone A5 reaches an intracellular target concentration of up to 10 nM. Although this corresponds to approximately 4% of all cellular mRNA, the turnover experiments indicated that this concentration is still at the low end of what could effectively catalyze a reaction (albeit with only 15% yield). In a crowded cellular environment where competing sequences are present, this may not be enough. Of note, other groups have successfully reported the application of templated azide reduction chemistries in living cells.[68–70] However, these studies either aimed at uncaging fluorescent dyes or employed self-immolative pyridinium or azidobenzyl linkers, which react significantly faster ($k_{app} = 138 \times 10^{-3}$ s^{-1}) than aliphatic azides ($k_{app} \approx 1 \times 10^{-3}$ s^{-1}) and produce much higher turnover.[43] The authors of these studies also highlighted the importance of the available template concentrations. Gorska et al. successfully used a phosphine-based reaction system on a highly expressed miRNA-21 template in MCF-7 cells but could not confirm a reaction in HeLa cells.[68] From RT-qPCR studies, the absolute copy numbers in these cell lines are known: MCF-7 strongly expresses miRNA-21 (>33 000 copies per cell; approximately 100–300 nM),[71] whereas HeLa has reduced (but still high) levels (approximately 12 000 copies per cell).[72] The expression level of XIAP mRNA in HEK XIAP A5 (14 200 copies per cell) is similar to the one of miRNA-21 in HeLa, which did not yield fluorescence in the templated reaction of Gorska et al.

Our experiments involving coelectroporated template point to another possibility. The 2′OMe-modified RNA template was used in micromolar concentration. Furthermore, 2′OMe-RNA is relatively stable against degradation by nucleases, and the affinity for PNA is higher than that of RNA for PNA. In spite of these beneficial properties, UPLC analysis of extracted probes revealed that the templated reaction did not occur in a cellular context. Perhaps, SMC-PNA probes are sequestered in the intracellular environment upon interaction with proteins or intracellular compartments. In previous work, we noticed a high unspecific cytotoxicity of SMC-PNA-CPP conjugates that we did not observe with PNA-CPP conjugates.[54] This effect may be due to the SMC's hydrophobicity.

5 | CONCLUSION

In summary, our investigations demonstrated how the unmasking of a masked SMC can be put under the control of a nucleic template. Using a set of two PNA conjugates, one bearing an azido-modified SMC and the other providing a reducing agent, we showed that synthetic RNA templates trigger the formation of an amino-SMC. We compared two PNA-linked reducing agents: (i) dimethyltriscarboxyethylphosphine and (ii) $Ru(bpy)_2(mcbpy)$. The latter afforded higher rates, yields, and turnover in template. The experiments revealed that 10 nM template was sufficient to trigger the formation of approximately 135 nM amino-SMC-PNA. For an evaluation of the templated azido-SMC reduction system *in cellulo*, a stable HEK 293 cell line was generated, which overexpressed a truncated, non-functional form of XIAP mRNA. Quantitative PCR suggested an intracellular template concentration of approximately

17 nM, which was deemed sufficient for further experiments. However, a successful transfer of the templated reaction system into living cells could not be demonstrated. The $Ru(bpy)_2(mcbpy)$ complex proved to be phototoxic, and the combined treatment of HEK XIAP cells with Ru(II)- and N_3-SMC probe did not result in a greater viability loss than treatment with Ru(II)-PNA alone or the combination with a scrambled N_3-SMC-PNA control. Efforts to isolate the product using a biotinylated probe and magnetic streptavidin-coated beads showed no intracellular product formation. A control experiment in total cellular RNA isolate revealed that the templated reaction can in principle proceed in a complex system with competing sequences being present; however, the mixture had to be spiked with 1 μM synthetic target. It was concluded that either the requirements regarding the template concentration are much higher in a crowded environment or the overexpressed sequence is inaccessible for the probes. Considering the lack of reactivity that was observed when reactive probes were coelectroporated with synthetic templates, it is also conceivable that the hydrophobicity of SMC-PNA conjugates impedes reactions in the intracellular context.

For a given cell target, the concentration and structure of the targeted RNA set unalterable barriers. On the contrary, the drug-like molecule activated or formed by the envisaged RNA-templated reaction is only limited by the imagination of the researcher. Considering the results obtained in this study, the focus should be set on compounds that avoid a high hydrophobicity and provide high bioactivity in the low nanomolar or even subnanomolar range. In future scenarios, PNA-based RNA recognition units may be replaced by oligonucleotide strands. Though PNA seems to facilitate turnover, oligonucleotide-based systems have higher solubility, and delivery into cells is easier. On these grounds, the science fiction idea of a gene expression specific synthesis of drugs inside disease cells is still a valid research objective.

ACKNOWLEDGEMENTS

This work was funded by the European Research Council's Horizon 2020 programme (ERC AdG 669628, TRIGGDRUG). The authors thank Dr. Dhana Friedrich and Prof. Alexander Löwer (Technical University Darmstadt, Darmstadt, Germany) for providing the mCherry-Ftag plasmid. Open Access funding enabled and organized by Projekt DEAL.

CONFLICT OF INTEREST

The authors have declared no conflict of interest.

ORCID

Peter Bou-Dib https://orcid.org/0000-0002-7146-8271
Oliver Seitz https://orcid.org/0000-0003-0611-4810

REFERENCES

1. Santos R, Ursu O, Gaulton A, et al. A comprehensive map of molecular drug targets. *Nat Rev Drug Discov*. 2017;16(1):19-34. doi:10.1038/nrd.2016.230
2. Gorska K, Winssinger N. Reactions templated by nucleic acids: more ways to translate oligonucleotide-based instructions into emerging function. *Angew Chem Int Ed*. 2013;52(27):6820-6843. doi:10.1002/anie.201208460
3. Di Pisa M, Seitz O. Nucleic acid templated reactions for chemical biology. *ChemMedChem*. 2017;12(12):872-882. doi:10.1002/cmdc.201700266
4. Ma ZC, Taylor JS. Nucleic acid-triggered catalytic drug release. *Proc Natl Acad Sci U S A*. 2000;97(21):11159-11163. doi:10.1073/pnas.97.21.11159
5. Silverman AP, Kool ET. Detecting RNA and DNA with templated chemical reactions. *Chem Rev*. 2006;106(9):3775-3789. doi:10.1021/cr050057+
6. Rossetti M, Bertucci A, Patiño T, Baranda L, Porchetta A. Programming DNA-based systems through effective molarity enforced by biomolecular confinement. *Chem – Eur J*. 2020;26(44):9826-9834. doi:10.1002/chem.202001660
7. Madsen M, Gothelf KV. Chemistries for DNA nanotechnology. *Chem Rev*. 2019;119(10):6384-6458. doi:10.1021/acs.chemrev.8b00570
8. Gartner ZJ, Tse BN, Grubina R, Doyon JB, Snyder TM, Liu DR. DNA-templated organic synthesis and selection of a library of macrocycles. *Science*. 2004;305(5690):1601-1605. doi:10.1126/science.1102629
9. Neri D, Lerner RA. DNA-encoded chemical libraries: a selection system based on endowing organic compounds with amplifiable information. *Annu Rev Biochem*. 2018;87(1):479-502. doi:10.1146/annurev-biochem-062917-012550
10. Saarbach J, Sabale PM, Winssinger N. Peptide nucleic acid (PNA) and its applications in chemical biology, diagnostics, and therapeutics. *Curr Opin Chem Biol*. 2019;52:112-124. doi:10.1016/j.cbpa.2019.06.006
11. Nielsen PE, Egholm M, Berg RH, Buchardt O. Sequence-selective recognition of DNA by strand displacement with a thymine-substituted polyamide. *Science*. 1991;254(5037):1497-1500. doi:10.1126/science.1962210
12. Egholm M, Buchardt O, Christensen L, et al. Pna hybridizes to complementary oligonucleotides obeying the Watson-crick hydrogen-bonding rules. *Nature*. 1993;365(6446):566-568. doi:10.1038/365566a0
13. Wehland JD, Lygina AS, Kumar P, et al. Role of the transmembrane domain in SNARE protein mediated membrane fusion: peptide nucleic acid/peptide model systems. *Mol Biosyst*. 2016;12(9):2770-2776. doi:10.1039/C6MB00294C
14. Dickgiesser S, Rasche N, Nasu D, et al. Self-assembled hybrid aptamer-fc conjugates for targeted delivery: a modular chemoenzymatic approach. *ACS Chem Biol*. 2015;10(9):2158-2165. doi:10.1021/acschembio.5b00315
15. Lygina AS, Meyenberg K, Jahn R, Diederichsen U. Transmembrane domain peptide/peptide nucleic acid hybrid as a model of a snare protein in vesicle fusion. *Angew Chem Int Ed*. 2011;50(37):8597-8601. doi:10.1002/anie.201101951
16. Bohler C, Nielsen PE, Orgel LE. Template switching between Pna and Rna oligonucleotides. *Nature*. 1995;376(6541):578-581. doi:10.1038/376578a0
17. Ma ZC, Taylor JS. PNA-based RNA-triggered drug-releasing system. *Bioconjug Chem*. 2003;14(3):679-683. doi:10.1021/bc034013o
18. Mattes A, Seitz O. Sequence fidelity of a template-directed PNA-ligation reactionPNA= peptide nucleic acid.12. *Chem Commun*. 2001;(20):2050-2051. doi:10.1039/b106109g
19. Mattes A, Seitz O. Mass-spectrometric monitoring of a PNA-based ligation reaction for the multiplex detection of DNA single-nucleotide polymorphisms. *Angew Chem Int Ed*. 2001;40(17):3178-3181. doi:10.1002/1521-3773(20010903)40:173.0.CO;2-M
20. Cai JF, Li XX, Yue X, Taylor JS. Nucleic acid-triggered fluorescent probe activation by the staudinger reaction. *J Am Chem Soc*. 2004;126(50):16324-16325. doi:10.1021/ja0452626

21. Dawson PE, Muir TW, Clark-Lewis I, Kent SBH. Synthesis of proteins by native chemical ligation. *Science*. 1994;266(5186):776-779. doi:10.1126/science.7973629
22. Ficht S, Mattes A, Seitz O. Single-nucleotide-specific PNA-peptide ligation on synthetic and PCR DNA templates. *J Am Chem Soc*. 2004;126(32):9970-9981. doi:10.1021/ja048845o
23. Ficht S, Dose C, Seitz O. As fast and selective as enzymatic ligations: unpaired nucleobases increase the selectivity of DNA-controlled native chemical PNA ligation. *ChemBioChem*. 2005;6(11):2098-2103. doi:10.1002/cbic.200500229
24. Dose C, Ficht S, Seitz O. Reducing product inhibition in DNA-template-controlled ligation reactions. *Angew Chem Int Ed*. 2006;45(32):5369-5373. doi:10.1002/anie.200600464
25. Dose C, Seitz O. Single nucleotide specific detection of DNA by native chemical ligation of fluorescence labeled PNA-probes. *Biorg Med Chem*. 2008;16(1):65-77. doi:10.1016/j.bmc.2007.04.059
26. Grossmann TN, Seitz O. DNA-catalyzed transfer of a reporter group. *J Am Chem Soc*. 2006;128(49):15596-15597. doi:10.1021/ja0670097
27. Grossmann TN, Röglin L, Seitz O. Target-catalyzed transfer reactions for the amplified detection of RNA. *Angew Chem Int Ed*. 2008;47(37):7119-7122. doi:10.1002/anie.200801355
28. Grossmann TN, Seitz O. Nucleic acid templated reactions: consequences of probe reactivity and readout strategy for amplified signaling and sequence selectivity. *Chem – Eur J*. 2009;15(27):6723-6730. doi:10.1002/chem.200900025
29. Erben A, Grossmann TN, Seitz O. DNA-triggered synthesis and bioactivity of proapoptotic peptides. *Angew Chem Int Ed*. 2011;50(12):2828-2832. doi:10.1002/anie.201007103
30. Michaelis J, Maruyama A, Seitz O. Promoting strand exchange in a DNA-templated transfer reaction. *Chem Commun*. 2013;49(6):618-620. doi:10.1039/C2CC36162K
31. Roloff A, Seitz O. The role of reactivity in DNA templated native chemical PNA ligation during PCR. *Biorg Med Chem*. 2013;21(12):3458-3464. doi:10.1016/j.bmc.2013.04.064
32. Roloff A, Seitz O. Bioorthogonal reactions challenged: DNA templated native chemical ligation during PCR. *Chem Sci*. 2013;4(1):432-436. doi:10.1039/C2SC20961F
33. Roloff A, Seitz O. Reducing product inhibition in nucleic acid-templated ligation reactions: DNA-templated cyclization. *Chembiochem*. 2013;14(17):2322-2328. doi:10.1002/cbic.201300516
34. Houska R, Stutz MB, Seitz O. Expanding the scope of native chemical ligation–templated small molecule drug synthesis via benzanilide formation. *Chem Sci*. 2021;12(40):13450-13457. doi:10.1039/D1SC00513H
35. Grossmann TN, Strohbach A, Seitz O. Achieving turnover in DNA-templated reactions. *ChemBioChem*. 2008;9(14):2185-2192. doi:10.1002/cbic.200800290
36. Michaelis J, Roloff A, Seitz O. Amplification by nucleic acid-templated reactions. *Org Biomol Chem*. 2014;12(18):2821-2833. doi:10.1039/C4OB00096J
37. Vazquez O, Seitz O. Cytotoxic peptide-PNA conjugates obtained by RNA-programmed peptidyl transfer with turnover. *Chem Sci*. 2014;5(7):2850-2854. doi:10.1039/C4SC00299G
38. Di Pisa M, Hauser A, Seitz O. Maximizing output in RNA-programmed peptidyl-transfer reactions. *Chembiochem*. 2017;18(9):872-879. doi:10.1002/cbic.201600687
39. Chang L-H, Seitz O. RNA-templated chemical synthesis of proapoptotic L- and d-peptides. *Biorg Med Chem*. 2022;66:116786. doi:10.1016/j.bmc.2022.116786
40. Pianowski ZL, Winssinger N. Fluorescence-based detection of single nucleotide permutation in DNA via catalytically templated reaction. *Chem Commun*. 2007;3820-3822.
41. Gorska K, Manicardi A, Barluenga S, Winssinger N. DNA-templated release of functional molecules with an azide-reduction-triggered immolative linker. *Chem Commun*. 2011;47(15):4364-4366. doi:10.1039/c1cc10222b
42. Sadhu KK, Winssinger N. Detection of miRNA in live cells by using templated RuII-catalyzed unmasking of a fluorophore. *Chem – Eur J*. 2013;19(25):8182-8189. doi:10.1002/chem.201300060
43. Chang D, Lindberg E, Winssinger N. Critical analysis of rate constants and turnover frequency in nucleic acid-templated reactions: reaching terminal velocity. *J Am Chem Soc*. 2017;139(4):1444-1447. doi:10.1021/jacs.6b12764
44. Gluhacevic Von Krüchten D, Roth M, Seitz O. DNA-templated reactions with high catalytic efficiency achieved by a loss-of-affinity principle. *J Am Chem Soc*. 2022;144(24):10700-10704. doi:10.1021/jacs.2c03188
45. Roth M, Seitz O. A self-immolative molecular Beacon for amplified nucleic acid detection**. *Chem – Eur J*. 2021;27(57):14189-14194. doi:10.1002/chem.202102600
46. Sayers J, Payne RJ, Winssinger N. Peptide nucleic acid-templated selenocystine-selenoester ligation enables rapid miRNA detection. *Chem Sci*. 2018;9(4):896-903. doi:10.1039/C7SC02736B
47. Middel S, Panse CH, Nawratil S, Diederichsen U. Native chemical ligation directed by photocleavable peptide nucleic acid (PNA) templates. *ChemBioChem*. 2017;18(23):2328-2332. doi:10.1002/cbic.201700487
48. Altrichter Y, Schöller J, Seitz O. Toward conditional control of Smac mimetic activity by RNA-templated reduction of azidopeptides on PNA or 2′-OMe-RNA. *Biopolymers*. 2021;112(12):e23466. doi:10.1002/bip.23466
49. Sun HY, Nikolovska-Coleska Z, Yang CY, et al. Design of small-molecule peptidic and nonpeptidic Smac mimetics. *Acc Chem Res*. 2008;41(10):1264-1277. doi:10.1021/ar8000553
50. Fulda S, Vucic D. Targeting IAP proteins for therapeutic intervention in cancer. *Nat Rev Drug Discov*. 2012;11(2):109-124. doi:10.1038/nrd3627
51. Bai L, Smith DC, Wang S. Small-molecule SMAC mimetics as new cancer therapeutics. *Pharmacol Ther*. 2014;144(1):82-95. doi:10.1016/j.pharmthera.2014.05.007
52. Liu Z, Sun C, Olejniczak ET, et al. Structural basis for binding of Smac/DIABLO to the XIAP BIR3 domain. *Nature*. 2000;408(6815):1004-1008. doi:10.1038/35050006
53. Wu G, Chai J, Suber TL, et al. Structural basis of IAP recognition by Smac/DIABLO. *Nature*. 2000;408(6815):1008-1012. doi:10.1038/35050012
54. Altrichter Y, Seitz O. Simultaneous targeting of two master regulators of apoptosis with dual-action PNA– and DNA–peptide conjugates. *Bioconjug Chem*. 2020;31(8):1928-1937. doi:10.1021/acs.bioconjchem.0c00284
55. Chamiolo J, Fang GM, Hövelmann F, et al. Comparing agent-based delivery of DNA and PNA forced intercalation (FIT) probes for multicolor mRNA imaging. *ChemBioChem*. 2019;20(4):595-604. doi:10.1002/cbic.201800526
56. Varfolomeev E, Blankenship JW, Wayson SM, et al. IAP antagonists induce autoubiquitination of c-IAPs, NF-κB activation, and TNFα-dependent apoptosis. *Cell*. 2007;131(4):669-681. doi:10.1016/j.cell.2007.10.030
57. Chai J, Du C, Wu JW, Kyin S, Wang X, Shi Y. Structural and biochemical basis of apoptotic activation by Smac/DIABLO. *Nature*. 2000;406(6798):855-862. doi:10.1038/35022514
58. Kipp RA, Case MA, Wist AD, et al. Molecular targeting of inhibitor of apoptosis proteins based on small molecule mimics of natural binding partners. *Biochemistry*. 2002;41(23):7344-7349. doi:10.1021/bi0121454
59. Yang QH, Du C. Smac/DIABLO selectively reduces the levels of c-IAP1 and c-IAP2 but not that of XIAP and Livin in HeLa cells. *J Biol Chem*. 2004;279(17):16963-16970. doi:10.1074/jbc.M401253200

60. Vince JE, Wong WWL, Khan N, et al. IAP antagonists target cIAP1 to induce TNFα-dependent apoptosis. *Cell*. 2007;131(4):682-693. doi:10.1016/j.cell.2007.10.037
61. Oost TK, Sun C, Armstrong RC, et al. Discovery of potent antagonists of the antiapoptotic protein XIAP for the treatment of cancer. *J Med Chem*. 2004;47(18):4417-4426. doi:10.1021/jm040037k
62. Lacasse EC, Kandimalla ER, Winocour P, et al. Application of XIAP antisense to cancer and other proliferative disorders: development of AEG35156/GEM640. *Ann N Y Acad Sci*. 2005;1058(1):215-234. doi:10.1196/annals.1359.032
63. Feng Y, Zhang N, Jacobs KM, et al. Polarization imaging and classification of Jurkat T and Ramos B cells using a flow cytometer. *Cytometry a*. 2014;85(9):817-826. doi:10.1002/cyto.a.22504
64. Stepanenko AA, Dmitrenko VV. HEK293 in cell biology and cancer research: phenotype, karyotype, tumorigenicity, and stress-induced genome-phenotype evolution. *Gene*. 2015;569(2):182-190. doi:10.1016/j.gene.2015.05.065
65. Mateus A, Matsson P, Artursson P. Rapid measurement of intracellular unbound drug concentrations. *Mol Pharm*. 2013;10(6):2467-2478. doi:10.1021/mp4000822
66. McClorey G, Banerjee S. Cell-penetrating peptides to enhance delivery of oligonucleotide-based therapeutics. *Biomedicine*. 2018;6(2):6. doi:*10.3390/biomedicines6020051*
67. Fransen JH, Dieker JW, Hilbrands LB, Berden JH, Van Der Vlag J. Synchronized turbo apoptosis induced by cold-shock. *Apoptosis*. 2011;16(1):86-93. doi:10.1007/s10495-010-0546-0
68. Gorska K, Keklikoglou I, Tschulena U, Winssinger N. Rapid fluorescence imaging of miRNAs in human cells using templated Staudinger reaction. *Chem Sci*. 2011;2(10):1969-1975. doi:10.1039/c1sc00216c
69. Shibata A, Ito Y, Abe H. RNA-templated molecule release induced protein expression in bacterial cells. *Chem Commun*. 2013;49(3):270-272. doi:10.1039/C2CC37826D
70. Holtzer L, Oleinich I, Anzola M, et al. Nucleic acid templated chemical reaction in a live vertebrate. *ACS Cent Sci*. 2016;2(6):394-400. doi:10.1021/acscentsci.6b00054
71. Guzman N, Agarwal K, Asthagiri D, et al. Breast cancer-specific miR signature unique to extracellular vesicles includes microRNA-like tRNA fragments. *Mol Cancer Res*. 2015;13(5):891-901. doi:10.1158/1541-7786.MCR-14-0533
72. Lim LP, Lau NC, Weinstein EG, et al. The microRNAs of *Caenorhabditis elegans*. *Genes Dev*. 2003;17(8):991-1008. doi:10.1101/gad.1074403

SUPPORTING INFORMATION

Additional supporting information can be found online in the Supporting Information section at the end of this article.

How to cite this article: Altrichter Y, Bou-Dib P, Kuznia C, Seitz O. Towards a templated reaction that translates RNA in cells into a proaptotic peptide-PNA conjugate. *J Pept Sci*. 2023;29(7):e3477. doi:10.1002/psc.3477